Materials Research. 2025; 28(suppl. 1): e20250090
DOI: https://doi.org/10.1590/1980-5373-MR-2025-0090

Microstructure Analysis of Ti–6Al–4V Alloy with TBC after Cyclic Oxidation for Aerospace Applications

Renata Jesuina Takahashi*[a], *Leonardo Henrique Fazan*[a], *Renato Baldan*[b], *Danieli Aparecida Pereira Reis*[a]

[a]*Universidade Federal de São Paulo (UNIFESP), Instituto de Ciência e Tecnologia, São José dos Campos, SP, Brasil.*
[b]*Universidade Estadual Paulista (UNESP), Campus de Itapeva, Itapeva, SP, Brasil.*

Received: January 10, 2025; Revised: July 01, 2025; Accepted: July 03, 2025

The application of thermal barrier coatings (TBC) on titanium alloys has been widely used in aircraft turbines to maintain their properties such as low density, mechanical strength, while also enabling higher operational temperatures and thermal efficiency. Corrosion and hot oxidation damage the TBC, which consist of a metallic substrate, a metallic coating (bond coat, BC), a thermally grown oxide (TGO), and a ceramic topcoat. This study assessed the oxidation behavior of Ti-6Al-4V with and without BC and TBC. Oxidation tests were conducted cyclically in air at temperatures of 500, 600, and 800 °C in an automatic furnace, in which each cycle consisted of 60 minutes at the target temperature followed by 10 minutes at room temperature. After 100 thermal cycles, the samples were analyzed using scanning electron microscopy (SEM), optical microscopy (OM), and X-ray diffraction (XRD). With increasing temperature, the uncoated Ti-6Al-4V alloy showed the formation of titanium oxides on the surface and an approximate 20% increase in grain size. In contrast, the TBC system demonstrated greater durability under high temperature conditions and showed no evidence of delamination.

Keywords: *Ti-6Al-4V alloy, TBC, Cyclic oxidation.*

1. Introduction

In the aerospace industry, surface treatments and coatings have long been used in various aircraft structures and components, which rely on these technologies to safeguard against a range of degradation mechanisms[1]. Thermal barrier coatings (TBC) have experienced significant advancements, leading to substantial improvements in turbine efficiency. These advancements have enabled higher operating temperatures, owing to the application of refractory oxide ceramic coatings, which protect metal turbine blades from thermal cycling and high heat flux[2-4].

The Ti-6Al-4V alloy was initially unable to meet the demands of high-temperature environments due to its insufficient oxidation resistance. However, the incorporation of a TBC system onto this alloy has raised its operational temperature capability by more than 400 °C[5]. Figure 1 shows a TBC system, which can be considered an integrated material system composed of several layers: a metal substrate, a metallic bond coat (BC), a thermally grown oxide (TGO), and a ceramic topcoat (TC)[6,7]. TBC system performance depends on the combined and individual properties of its constituent layers. The mechanical strength of the substrate predominates, along with the oxidation resistance of the BC and the thermal cycling resistance of the TC. The TGO layer promotes good adhesion between the metallic and ceramic materials, in which chemical incompatibility and thickness are factors for optimal performance[6,8].

The service life of a TBC system is ultimately limited by the integrity of its structure. TGO expansion is among the primary failure mechanisms, which is a significant contributing factor to the failure of TBC systems due to oxidation. This occurs because of the ionic permeability of the topcoat under operational conditions[9,10]. The TGO layer thickness is generally regarded as a critical factor that influences the lifespan of a TBC system, particularly under the influence of thermal cycling and thermal stresses during service[9-15].

In aerospace applications, the Ti-6Al-4V alloy experiences the effects of mechanical stress (creep) and repeated thermal cycling under high temperatures[16-22]. The literature holds many study on creep in titanium alloys with TBC. However, the cyclic oxidation behavior of Ti-6Al-4V alloy has not been as extensively studied as its isothermal oxidation performance[23-27]. The cyclic oxidation resistance is therefore as crucial as isothermal oxidation resistance, as thermal shock phenomena often occur in applications. These phenomena can lead to cracking and fragmentation of oxide scales, compromising the integrity of the material and reducing its performance.

In this context, cyclic oxidation tests of titanium alloys with NiCrAlY bond coatings and TBCs deposited by air plasma spray (APS) are scarcely reported in the literature. The microstructural evolution following cyclic oxidation tests at these temperatures can provide important insights into the performance of the

*e-mail: danieli.reis@unifesp.br
Associate Editor: Igor Vasconcelos.
Editor-in-Chief: Luiz Antonio Pessan.

TBC system, particularly regarding its effectiveness in offering thermal and chemical protection to the titanium alloy. A stable and unaltered microstructure contributes to maintaining the mechanical integrity required for aerospace turbine blade applications. This study aimed to investigate the microstructure of Ti alloy after cyclic oxidation tests, focusing on the behavior of BC and TBC layers at 500, 600, and 800 °C. The samples were analyzed using scanning electron microscopy (SEM), energy dispersive spectroscopy (EDS) elemental mapping, and X-ray diffraction (XRD) techniques to compare the effects of oxidation at each test temperature.

2. Materials and Method

The Ti-6Al-4V Grade 5 alloy samples were fabricated in the form of discs with a 3.17 mm in diameter and 2 mm thick. The thermal barrier coating (TBC) system comprised a bond coat (BC) of NiCrAlY (AMDRY 962) and a top coat (TC) of yttria-stabilized zirconia containing 8 wt% yttria (8YSZ – Metco 204NS-G). Both layers were deposited using a commercial air plasma spray (APS) process on titanium alloy. Figure 2 shows the surfaces of the Ti-6Al-4V alloy coated with the BC and TBC deposited by APS.

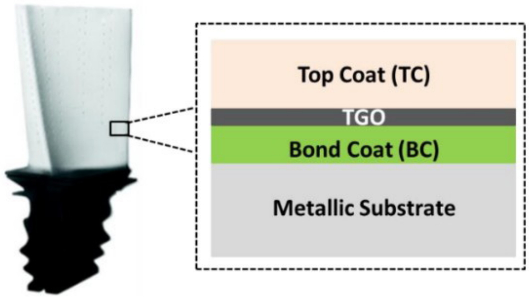

Figura 1. Schematic of a thermal barrier system for application on airplane engine blades[7].

Cyclic oxidation tests were conducted in an automatic horizontal tubular furnace (FT-1200/H/OC/CLP) at temperatures of 500, 600, and 800 °C, with 100 cycles. Each cycle consisted of 60 minutes inside the furnace and 10 minutes at room temperature. The tested samples were examined in three different conditions: Ti-6Al-4V alloy without coating, with BC and with TBC. Table 1 shows the mean thicknesses of the BC and TBC layers subjected to the cyclic oxidation test.

The isothermal oxidation behavior of both uncoated and TBC samples was investigated by thermogravimetric analysis (TGA) and discontinuous oxidation tests. The TGA was performed at 600 °C for 7 hours in a synthetic air atmosphere consisting of 20% O_2 and 80% N_2, with a constant flow rate of 20 mL/min. The discontinuous oxidation test was conducted in a muffle furnace (EDG, W-Three) with a CPU-10P-LCD2 controller, and mass measurements were obtained using a thermobalance (Netzsch, TG 209 F12) for a total time of approximately 130 hours. Both methods provided data on mass gain as a function of time.

The metallographic preparation was conducted by precision cross-sectioning of the samples using a precision cut-off machine (Struers, Minitom). Subsequently, the specimens were ground with silicon carbide abrasive papers (320, 400, 600, 800, and 1200 mesh). Final polishing was performed using 6 μm and 3 μm diamond pastes and finished with colloidal silica. The microstructure was revealed using Kroll's reagent, composed of 5 mL of HNO_3, 3 mL of HF, and 92 mL of distilled water.

The microstructural comparison and the visual integrity of the coatings were characterized using scanning electron microscopy (SEM) (Tescan, FE SEM MIRA 3) with coupled energy dispersive spectroscopy (EDS) (Oxford Instruments, X Max M). The optical microscopy (Olympus BX53M), equipped with the PRECiV Pro imaging software, was used to perform grain size analysis in accordance with ASTM E112-13[28]. Phase analyses were performed using X-ray diffraction (XRD) (Rigaku, Ultima IV) with a CuKα radiation source (PANalytical model X'Pert PRO Multipurpose

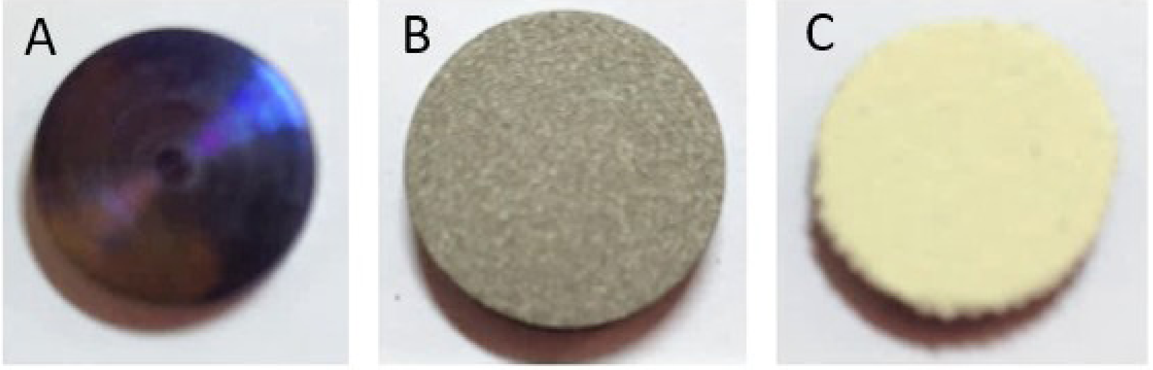

Figura 2. Surface of the samples with a diameter of 3.17 mm and a thickness of 2.00 mm were prepared for cyclic oxidation tests. A) Ti-6Al-4V. B) BC by APS deposition. C) TBC by APS deposition.

Table 1. Mean thicknesses of the BC and TBC samples before the cyclic oxidation test.

	500 °C	600 °C	800 °C
BC	105.77 ± 28.85	184.61 ± 38.46	161.54 ± 7.70
TBC	464.29 ± 39.68	458.33 ± 25.0	479.17 ± 18.75

Diffractometer). The data for each phase were analyzed by diffraction patterns (PANalytical HighScore software), and the results are based on the comparison of the titanium alloy microstructure as the oxidation test temperature increases.

3. Results and Discussion

Figure 3 shows the microstructure of the Ti-6Al-4V alloy subjected to cyclic oxidation testing. Note that the bimodal microstructure was preserved with an increase in the oxidation after 100 cycles oxidations by MO. A) 500 °C. B) 600 °C. C) 800 °C.

Figure 4 shows the microstructure of the titanium alloy with the BC. Notably, the coatings remained well-adhered to the metallic substrate, thereby preserving the bimodal microstructure of the titanium alloy.

Figure 5 shows the microstructure of the TBC and the titanium alloy in the centre of the sample. The TBC showed

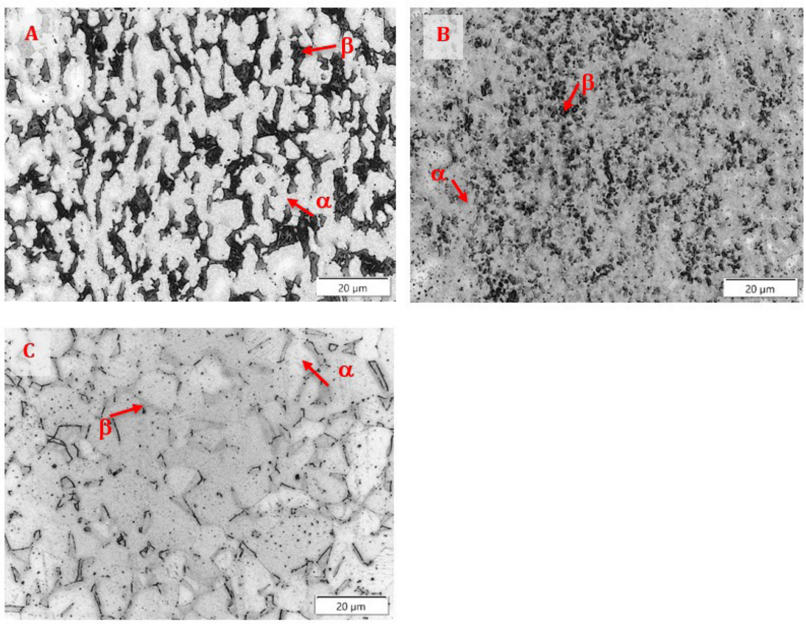

Figura 3. Microstructure of the Ti-6Al-4V after 100 cycles oxidations by MO. A) 500 °C. B) 600 °C. C) 800 °C.

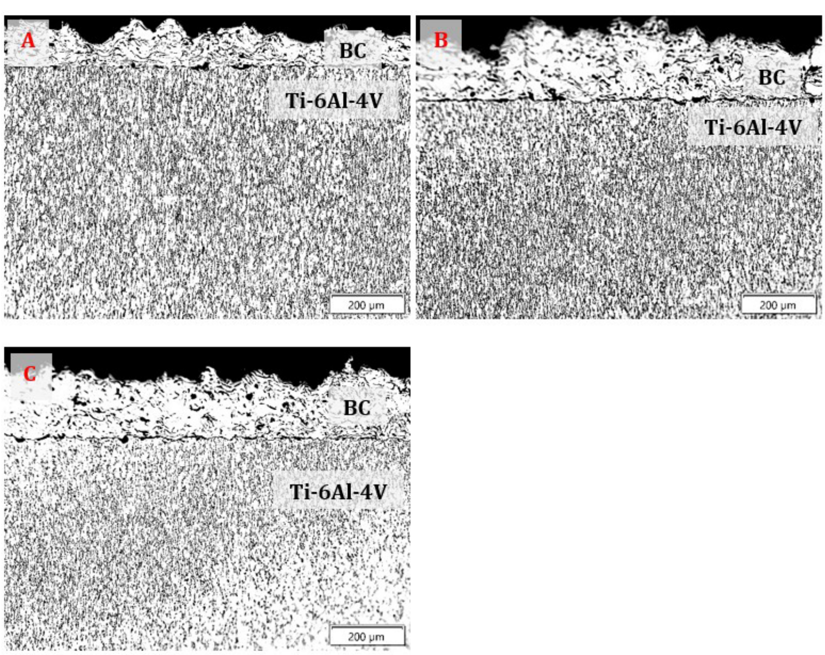

Figura 4. Microstructure of the Ti-6Al-4V with BC after 100 cycles oxidations by MO. A) 500 °C. B) 600 °C. C) 800 °C.

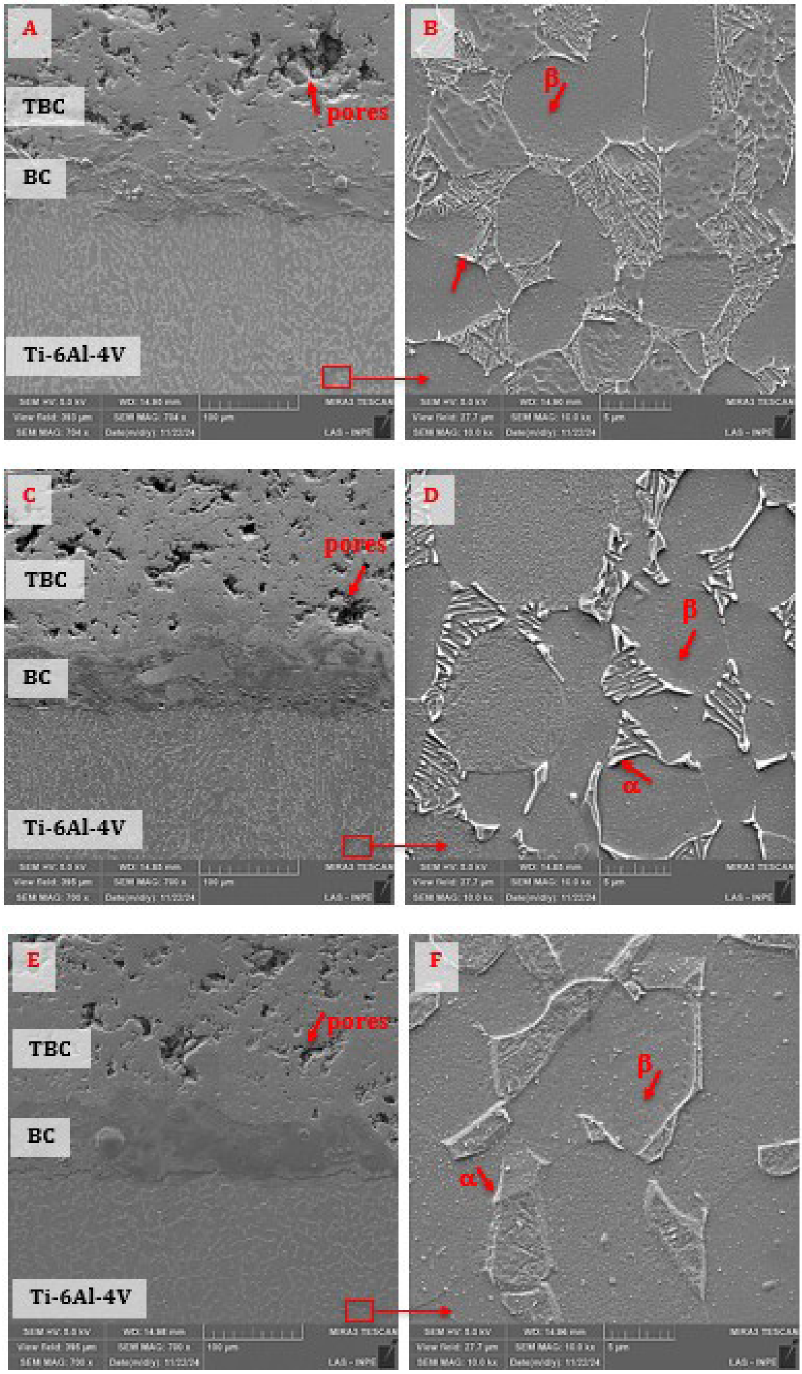

Figura 5. Microstructure of the Ti-6Al-4V with TBC after 100 cycles oxidations by MEV. A) 500 °C. B) Ti-6Al-4V at 500 °C. C) 600 °C. D) Ti-6Al-4V at 600 °C. E) 800 °C. F) Ti-6Al-4V at 600 °C.

no signs of delamination and remained intact after 100 thermal cycles. A bimodal microstructure consisting of α and β phases was identified. Although the TBC layer remained adherent, regions of increased porosity were observed, likely resulting from thermal exposure and the stresses induced by cyclic loading, thus, increasing temperature lead to grain grown. Porosity was estimated using ImageJ software by calculating the area fraction corresponding to pores in the micrographs (Figures 5A, 5C and 5E), and the measured porosity values were 10.5%, 11.3%, and 13.1% for the Ti-6Al-4V, BC, and TBC samples, respectively.

Figure 6 shows grain size variation as a function of temperature. A similar grain growth trend is observed in all samples, but it is noteworthy that the presence of the coatings can slow down grain growth. The TBC application demonstrated superior effectiveness compared to the bond coat. The grain size of the Ti-6Al-4V alloy becomes coarser with increasing temperature, as observed (Figure 3) in the

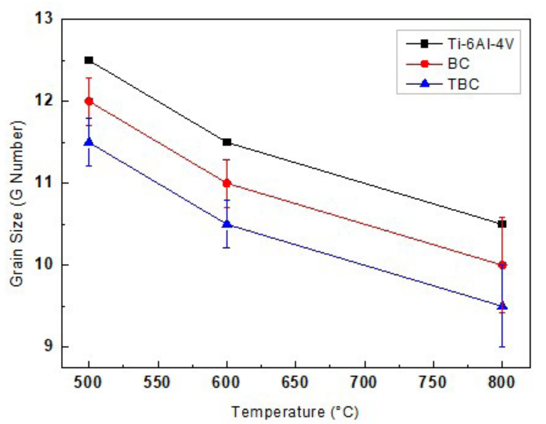

Figura 6. The grain size (G number according to ASTM E112-1328[28]) of the Ti-6Al-4V with BC and TBC after 100 cycles oxidations at 500 °C, 600 °C and 800 °C.

areas that correspond to the α-phase (lighter areas) and β-phase (darker areas).

Figure 7 also shows the integrity and good adhesion of the TBC in the EDS mapping analysis. Table 2 shows the weight percentages of the chemical elements identified by the EDS analysis, along with their respective standard deviations.

The chemical elements comprising the TBC coatings were identified via EDS analysis (Figure 7). The TBC integrity is evidenced by the homogeneous spatial distribution of the chemical elements within each layer, enabling the identification of the interfaces between them. The well-defined interfaces suggest good adhesion between the layers, with no signs of significant interdiffusion or delamination, even after the cyclic oxidation test.

The presence of oxygen was more prominent following the cyclic oxidation test at 800 °C (Figure 7 and Table 2), indicating oxygen ingress through the TBC pores (Figures 5A, 5C and 5E), which was further enhanced

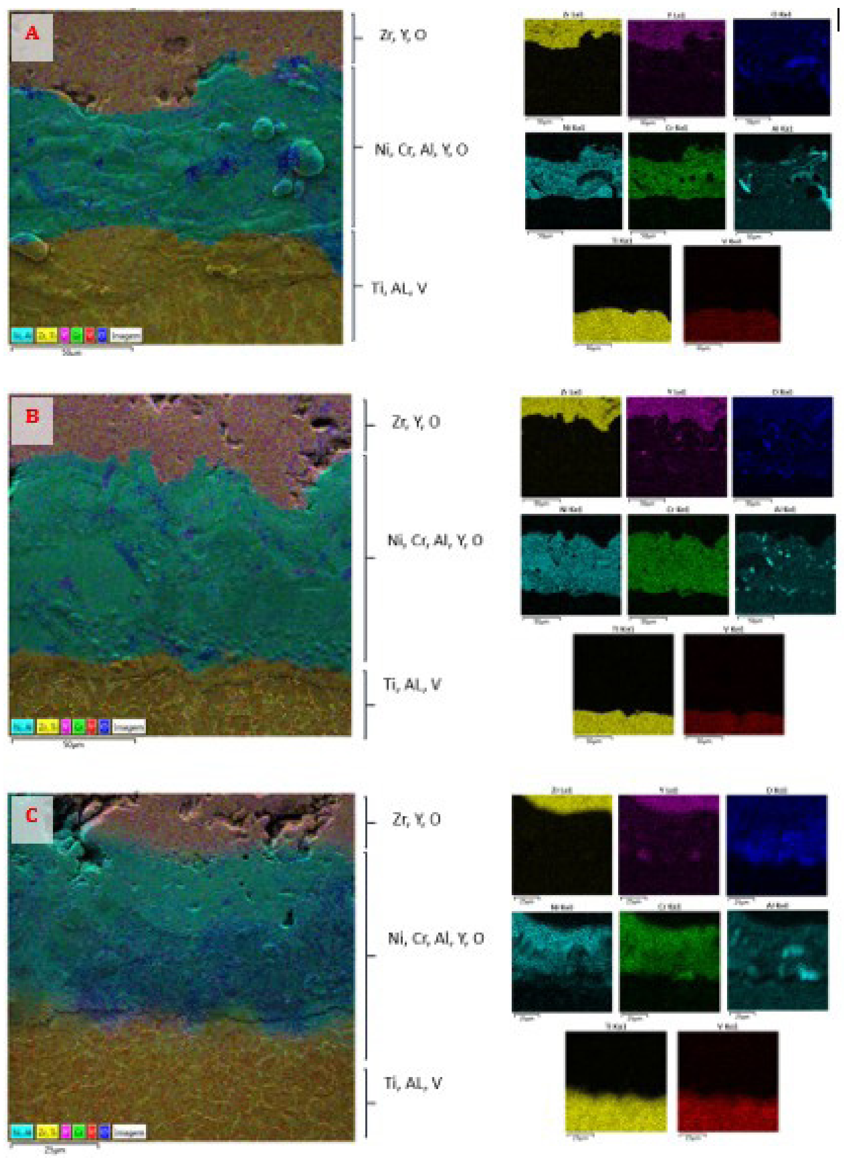

Figura 7. EDS map analysis of the Ti-6Al-4V with TBC after 100 cycles oxidations. A) 500 °C. B) 600 °C. C) 800 °C.

during thermal cycling. A similar trend was observed for aluminum, in which the possible diffusion and interaction between aluminum from the adjacent BC layer and oxygen caused TGO growth. Accordingly, Table 3 shows that the mean thicknesses of TGO after cyclic oxidation in the TBC samples, which prove the more pronounced TGO formation in the samples subjected to higher temperatures.

The oxidation phenomenon in TBCs occurs by two basic mechanisms. The first one occurs when oxygen ingresses through defects such as voids, cracks, and porosity within the TC, while the second is driven by oxygen diffusion via the inherent ionic conductivity of the yttria-stabilized zirconia (YSZ) TC[25]. Air plasma sprayed top is composed of overlapping splats oriented parallel to the substrate, which are characterized by poor inter-splat bonding, intra-splat microcracks, and the presence of large, irregularly shaped pores[26,27]. Oxygen transport through the top coat leads to oxidation of the bond coat during high-temperature operation, which predominantly result in the formation of aluminum oxides[11]. Under the operating conditions of a TBC in a gas turbine, oxygen transport through the top coat by gas permeation is predicted to dominate over diffusion[25].

The degradation of oxidation resistance in the coating in this mechanism is associated with the depletion of aluminum due to oxide spallation and interdiffusion between the BC and the Ni-based superalloy, forming a TGO. Oxides containing elements such as Co, Cr, Ni, Ta, and Ti can lead to severe spallation during cyclic oxidation after approximately 160 hours at 1050 °C. Moreover, the outward diffusion of substrate elements, particularly titanium, accelerates the spallation of the oxide scale[29].

The TGO layer represents the most vulnerable region of the TBC system. In the literature[30], cyclic oxidation tests on TBCs (8YSZ/$Gd_2Zr_2O_7$) applied to Inconel 718 by EB-PVD at 1100 °C for varying periods showed that TGO growth during thermal cycles and delamination occurred in this area. The thermal expansion mismatch between the layers is likely a primary factor contributing to delamination. The premature formation of cracks during thermal cycling was attributed to the low coefficient of thermal expansion and low fracture toughness of ceramics, which were identified as key factors enhancing the oxidation resistance of TBCs during thermal cycling.

In Ti-6Al-4V alloys with BC deposited by APS, mixed Al_2O_3/TiO_2 oxide scales provide less protection than pure Al_2O_3 scales, which occurs because TiO_2 grows at a faster rate than Al_2O_3 at high temperatures. The higher TiO_2 grown rate is attributed to its characteristic channel structure, which facilitates oxygen transport through fast diffusion pathways[31].

The investigation of internal elemental diffusion in titanium was conducted to minimize the possibility of loss of oxidation resistance. As estimated by EDS analysis (Table 2), the oxygen weight percentage increased with the rise in temperature, as diffusion is thermally activated. In addition, Figure 8 shows the X-ray diffraction (XRD) analysis, which was used to confirm the phases on the surface of the samples.

The XRD analysis enabled the identification of the crystalline phases on the surface of all samples. For the uncoated Ti-6Al-4V alloy, a variety of titanium oxides were detected on the surface with increasing temperature (Figure 8A) and the diffractograms revealed a predominant presence of the titanium (01-089-5009) and titanium oxides (TiO_2, 01-073-1116; TiO, 00-043-1295; Ti_3O, 01-073-1583). The phase identification was conducted via comparison with standard databases (ICSD Pattern), and the corresponding reference codes are provided.

In contrast, the samples coated with the BC and TBC did not show significant changes in their XRD patterns with increasing temperature, further confirming the protective role of the coatings in mitigating oxidation of the titanium alloy. The diffractograms revealed a predominant presence of the AlNi phase for the BC. In the case of the TBC, the dominant phases were cubic ZrO_2 and ZrOYO.

The cyclic oxidation behavior of plasma surface chromium plating on Ti–6Al–4V was investigated in air at temperatures of 650 °C, 750 °C, and 850 °C. Each cycle consisted of one hour at the target temperature, followed by ten minutes of cooling down to 60 °C, and the results showed that the formation of $Ti(Cr,Al)_2$ phase layers caused the fragmentation of the oxide scales at 750 °C and 850 °C. However, the cyclic oxidation resistance remained superior to the NiCrAlY thermal barrier coating one[32].

Ti–6Al–4V alloys with different BC compositions, deposited via APS, underwent cyclic oxidation tests at 800 °C for 100 cycles. Each cycle consisted of one hour in the furnace, followed by ten minutes in air, and the results demonstrated

Table 2. Weight percentage of the EDS analysis of the Ti-6Al-4V with TBC after 100 cycles oxidations.

	500 °C	600 °C	800 °C
Ti	21.4 ± 0.1	30.7 ± 0.2	34.0 ± 0.2
Ni	35.3 ± 0.2	23.9 ± 0.2	21.4 ± 0.2
O	7.1 ± 0.1	13.2 ± 0.2	15.4 ± 0.2
Cr	13.8 ± 0.1	9.2 ± 0.1	12.7 ± 0.1
Al	6.6 ± 0.1	6.4 ± 0.1	7.9 ± 0.1
Zr	14.2 ± 0.2	14.1 ± 0.2	7.1 ± 0.2
V	0.7 ± 0.1	0.9 ± 0.1	1.0 ± 0.1
Y	1.0 ± 0.1	1.4 ± 0.1	0.4 ± 0.1

Table 3. Mean thicknesses of the TGO in TBC samples after the cyclic oxidation test.

	500 °C	600 °C	800 °C
TGO	4.79 ± 0.68	5.61 ± 1.14	6.16 ± 2.05

Table 4. Percentage mass gain obtained from thermogravimetric and discontinuous oxidation tests of Ti-6Al-4V and TBC at 600 °C[33].

	TGA (7h)	Discontinuous oxidation test (130 h)
Ti-6Al-4V	0.23	1.05
TBC	0.12	0.18

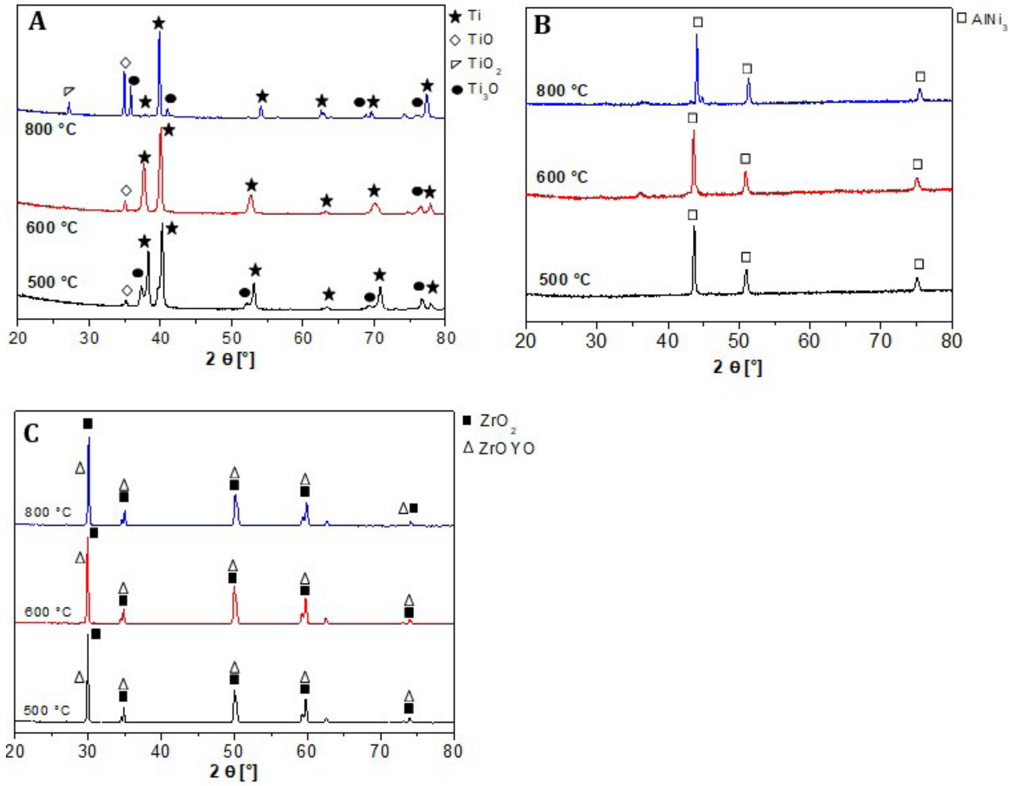

Figura 8. XRD analysis after 100 cycles oxidations at 500, 600 and 800 °C. A) Ti-6Al-4V. B) BC. C) TBC.

that the best oxidation resistance was achieved with NiCrAlY coatings, as the Ni_3Al phase enhances thermal stability. This is attributed to the fact that the Ni_3Al oxide acts more effectively as a barrier to oxygen diffusion as oxidation progresses[31]. Similarly, the samples with BC coatings exclusively showed the Ni_3Al phase (Figure 8B) across all test temperatures. Therefore, it is hypothesized that the BC contributed to good oxidation resistance, not only by the formation of the Ni_3Al phase, but also by ensuring the adhesion and integrity of the BC. A similar protective effect against thermal cycling was observed with the thermal barrier coating (TBC).

The mass gain after cyclic oxidation cycles is a challenge to determine due to the automation of the furnace and the temperature of the samples. In contrast, isothermal oxidation tests such as TGA allow for continuous monitoring of mass gain and the observation of a consistent trend over time at a fixed temperature. Figure 9 shows the mass gain behavior of the Ti-6Al-4V alloy samples and TBC samples at 600 °C.

Table 4 shows the percentage mass gain obtained from TGA and discontinuous oxidation tests at 600 °C.

In both analyses, the uncoated Ti-6Al-4V alloy exhibited the highest mass gain compared to the TBC samples. The presence of the TBC significantly enhanced the oxidation resistance of the alloy.

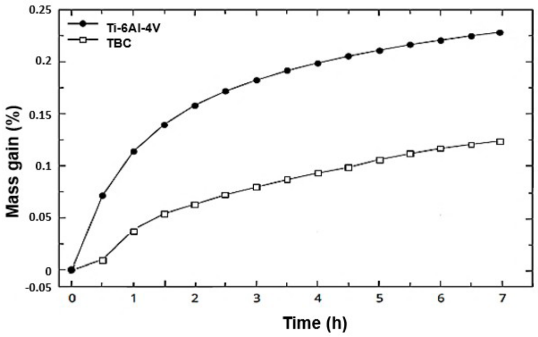

Figura 9. Thermogravimetric analysis of Ti-6Al-4V and TBC at 600 °C[33].

4. Conclusion

The oxidation of 100 thermal cycles at 500, 600, and 800 °C of the Ti-6Al-4V alloy, both with and without BC and TBC coatings, led to the following conclusions:

- The BC and TBC coatings were effective in protecting the titanium alloy against cyclic oxidation, as confirmed by microstructural analysis. The TBC

system showed greater durability against high-temperature degradation, and the grain growth of the titanium alloy with the TBC was reduced by approximately 20% compared to the uncoated alloy.
- The BC coating exclusively showed the Ni_3Al phase, which enhances the oxidation protection of the titanium alloy by forming a robust protective layer.
- The TBC microstructure showed a porosity of approximately 13%, remained intact and maintained adhesion to the Ti-6Al-4V alloy under all test conditions. The oxygen permeability through the TC may have facilitated the formation and growth of the TGO layer to a sufficient thickness, thereby contributing to the prevention of delamination between the layers.
- TGA analysis indicated the lowest mass gain in the TBC samples compared to the uncoated Ti-6Al-4V at 600 °C for seven hours, which confirms the protective effect of the coating.

5. Acknowledgments

This study was partially financed by the National Council for Scientific and Technological Development – CNPq (151989/2024-9). The authors are grateful to FAPESP and Finep.

6. References

1. Fernandes FAP, Baldan R, Malafaia AMS. Advanced corrosion and high-temperature protection through surface modification and coatings. Coatings. 2023;13(11):1940. http://doi.org/10.3390/coatings13111940.
2. Takahashi RJ, Assis JMK, Piorino F No, Reis DAP. Thermal conductivity study of ZrO2-YO1.5-NbO2.5 TBC. J Mater Res Technol. 2022;19:4932-8. http://doi.org/10.1016/j.jmrt.2022.07.037.
3. Clarke DR, Phillpot SR. Thermal barrier coating materials. Mater Today. 2005;8(6):22-9. http://doi.org/10.1016/S1369-7021(05)70934-2.
4. Almeida DS, Piorino F No, Henriques VAR, Assis JMK, Gonçalves PAR, Takahashi RJ, et al. Study of non-transformable t′-YSZ by addition of niobia for TBC application. Coatings. 2024;14(3):249. http://doi.org/10.3390/coatings14030249.
5. Inagaki I, Takechi T, Shirai Y, Ariyasu N. Application and features of titanium for the aerospace industry. Tokyo: Nippon Steel; 2014. (Nippon Steel & Sumitomo Metal Technical Report; 6).
6. Levi CG. Emerging materials and processes for thermal barrier systems. Curr Opin Solid State Mater Sci. 2004;8(1):77-91. http://doi.org/10.1016/j.cossms.2004.03.009.
7. Takahashi R, Assis J, Reis D. Microstructural characterization of zirconia co-doped with yttria and niobia by laser deposition on Ti-6Al-4V as a thermal barrier for application in turbines. SAE Technical Paper. 2018;36:0332. http://doi.org/10.4271/2018-36-0332.
8. Clarke DR, Levi CG. Materials design for the next generation thermal barrier coatings. Annu Rev Mater Res. 2003;33(1):383-417. http://doi.org/10.1146/annurev.matsci.33.011403.113718.
9. Doleker KM, Ozgurluk Y, Karaoglanli AC. TGO growth and kinetic study of single and double layered TBC systems. Surf Coat Tech. 2021;415:127135. http://doi.org/10.1016/j.surfcoat.2021.127135.
10. Zhu C, Li P, Wu XY. A study of the diffusion and pre-oxidation treatment on the formation of Al2O3ceramic scale on NiCrAlY bond-coat during initial oxidation process. Ceram Int. 2016;42(6):7708-16. http://doi.org/10.1016/j.ceramint.2016.01.185.
11. Takahashi RJ, Assis JMK, Piorino F No, Reis DAP. Heat treatment for TGO growth on NiCrAlY for TBC application. Mater Res Express. 2020;6(12):126442. http://doi.org/10.1088/2053-1591/ab6778.
12. Martena M, Botto D, Fino P, Sabbadini S, Gola MM, Badini C. Modelling of TBC system failure: stress distribution as a function of TGO thickness and thermal expansion mismatch. Eng Fail Anal. 2006;13(3):409-26. http://doi.org/10.1016/j.engfailanal.2004.12.027.
13. Dong H, Yang GJ, Li CXCJ, Luo XT, Li CXCJ. Effect of TGO thickness on thermal cyclic lifetime and failure mode of plasma-sprayed TBC s. J Am Ceram Soc. 2014;97(4):1226-32. http://doi.org/10.1111/jace.12868.
14. Shen Q, Yang L, Zhou YC, Wei YG, Wang NG. Models for predicting TGO growth to rough interface in TBCs. Surf Coat Tech. 2017;325:219-28. http://doi.org/10.1016/j.surfcoat.2017.06.001.
15. Chen WR, Wu X, Marple BR, Nagy DR, Patnaik PC. TGO growth behaviour in TBCs with APS and HVOF bond coats. Surf Coat Tech. 2008;202(12):2677-83. http://doi.org/10.1016/j.surfcoat.2007.09.042.
16. Sugahara T, Reis DAP, Briguente LANS, Yogi LM, Silva HR, Fonseca FB. Evaluation of heat treatment in creep of Ti-6Al-4V alloy. SAE Technical Paper. 2009;36:0136. http://doi.org/10.4271/2009-36-0136.
17. Freitas FE, Briguente FP, Reis AG, Vasconcelos G, Reis DAP. Investigation on the microstructure and creep behavior of laser remelted thermal barrier coating. Surf Coat Tech. 2019;369:257-64. http://doi.org/10.1016/j.surfcoat.2019.04.068.
18. Reis DAP, Silva CRM, Nono MCA, Barboza MJR, Piorino F No, Perez EAC. Plasma-sprayed coatings for oxidation protection on creep of the Ti–6Al–4V alloy. Mater High Temp. 2005;22(3):449-52. http://doi.org/10.3184/096034005782744227.
19. Barboza MJRR, Perez EACC, Medeiros MM, Reis DAPP, Nono MCAA, Piorino F No, et al. Creep behavior of Ti-6Al-4V and a comparison with titanium matrix composites. Mater Sci Eng A. 2006;428(1-2):319-26. http://doi.org/10.1016/j.msea.2006.05.089.
20. Reis DAP, Moura C No, Silva CRM, Barboza MJR, Piorino F No. Effect of coating on the creep behavior of the Ti-6Al-4V alloy. Mater Sci Eng A. 2008;486(1-2):421-6. http://doi.org/10.1016/j.msea.2007.09.024.
21. Briguente FP, Silva Briguente LAN, Reis DAP, Silva MM. Comparative study of creep resistance of a Ti-6Al-4V alloy with metallic and ceramic coatings. Mater Sci Forum. 2014;802:472-6. http://doi.org/10.4028/www.scientific.net/MSF.802.472.
22. Sugahara T, Reis DAP, Moura C No, Barboza MJR, Perez EAC, Piorino F No, et al. The effect of widmanstätten and equiaxed microstructures of Ti-6Al-4V on the oxidation rate and creep behavior. Mater Sci Forum. 2010;636–637:657-62. http://doi.org/10.4028/www.scientific.net/MSF.636-637.657.
23. Doleker KM, Karaoglanli AC, Ozgurluk Y, Kobayashi A. Performance of single YSZ, Gd2Zr2O7 and double-layered YSZ/Gd2Zr2O7 thermal barrier coatings in isothermal oxidation test conditions. Vacuum. 2020;177:109401. http://doi.org/10.1016/j.vacuum.2020.109401.
24. Jiang C, Chen J, Zhu Z. Novel structured spark plasma sintered thermal barrier coatings with high strain tolerance and oxidation resistance. Ceram Int. 2022;48(9):12271-80. http://doi.org/10.1016/j.ceramint.2022.01.088.
25. Fox AC, Clyne TW. Oxygen transport by gas permeation through the zirconia layer in plasma sprayed thermal barrier coatings. Surf Coat Tech. 2004;184(2-3):311-21. http://doi.org/10.1016/j.surfcoat.2003.10.018.
26. Nowak W, Naumenko D, Mor G, Mor F, Mack DE, Vassen R, et al. Effect of processing parameters on MCrAlY bondcoat roughness and lifetime of APS-TBC systems. Surf Coat Tech. 2014;260:82-9. http://doi.org/10.1016/j.surfcoat.2014.06.075.
27. Evans HE. Oxidation failure of TBC systems: an assessment of mechanisms. Surf Coat Tech. 2011;206(7):1512-21. http://doi.org/10.1016/j.surfcoat.2011.05.053.

28. ASTM: American Society for Testing and Materials. ASTM E112-13(2021): standard test methods for determining average grain size. West Conshohocken: ASTM; 2021. http://doi.org/10.1520/E0112-13R21.
29. Liang T, Guo H, Peng H, Gong S. Cyclic oxidation behavior of an EB-PVD CoCrAlY coating influenced by substrate/coating interdiffusion. Chin J Aeronauti. 2012;25(5):796-803. http://doi.org/10.1016/S1000-9361(11)60447-0.
30. Doleker KM, Ozgurluk Y, Ahlatci H, Karaoglanli AC. Evaluation of oxidation and thermal cyclic behavior of YSZ, $Gd_2Zr_2O_7$ and YSZ/$Gd_2Zr_2O_7$ TBCs. Surf Coat Tech. 2019;371:262-75. http://doi.org/10.1016/j.surfcoat.2018.11.055.
31. Choi BY, Liang J, Gao W. Correlation of microstructure and high temperature oxidation resistance of plasma sprayed NiCrAl, NiCrAlY, and TiAlO composite coatings on Ti-6Al-4V. Met Mater Int. 2005;11(6):499-503. http://doi.org/10.1007/BF03027500.
32. Wei DB, Zhang PZ, Yao ZJ, Zhou JT, Wei XF, Zhou P. Cyclic oxidation behavior of plasma surface chromising coating on titanium alloy Ti-6Al-4V. Appl Surf Sci. 2012;261:800-6. http://doi.org/10.1016/j.apsusc.2012.08.102.
33. Freitas FE, Reis AG, Oliveira AC, Reis DAP. Investigação da refusão por laser no recobrimento como forma de barreira térmica. In: 74º Congresso Anual da ABM; 2019; São Paulo. Anais. São Paulo: ABM; 2019. p. 3328-39. http://doi.org/10.5151/2594-5327-33531.

Data Availability

The entire dataset that supports the results of this study has been published within the article itself.